Solar Energy Materials & Solar Cells 149 (2016) 15–18

Contents lists available at ScienceDirect

Solar Energy Materials & Solar Cells

journal homepage: www.elsevier.com/locate/solmat

Demonstration of the operation principles of intermediate band solar cells at room temperature

E. López [a,*], A. Datas [a], I. Ramiro [a], P.G. Linares [a], E. Antolín [a], I. Artacho [a], A. Martí [a], A. Luque [a], Y. Shoji [b], T. Sogabe [b], A. Ogura [b], Y. Okada [b]

[a] Instituto de Energía Solar – Universidad Politécnica de Madrid ETSI Telecomunicación, Ciudad Universitaria sn, 28040 Madrid, Spain
[b] Research Center for Advanced Science and Technology (RCAST), The University of Tokyo, 4-6-1 Komaba, Meguro-ku, Tokyo 153-8904, Japan

ARTICLE INFO

Article history:
Received 23 June 2015
Received in revised form
9 December 2015
Accepted 27 December 2015

Keywords:
Intermediate band solar cells
InGaAs/AlGaAs quantum dots
Two-photon photocurrent
Voltage preservation

ABSTRACT

In this work we report, for the first time at room temperature, experimental results that prove, simultaneously in the same device, the two main physical principles involved in the operation of intermediate band solar cells: (1) the production of sub-bandgap photocurrent by two optical transitions through the intermediate band; (2) the generation of an output voltage which is not limited by the photon energy absorption threshold. These principles, which had always required cryogenic temperatures to be evidenced all together, are now demonstrated at room temperature on an intermediate band solar cell based on InAs quantum dots with $Al_{0.3}Ga_{0.7}As$ barriers.

1. Introduction

The structure of an intermediate band solar cell (IBSC) enables an increase of the photo-generated current, as a consequence of the reduction of the photon absorption energy threshold, without the output voltage of the cell being limited by this threshold. This break in the trade-off between current and voltage makes the efficiency limit of an IBSC surpasses the Shockley–Queisser (SQ) limit established for single gap solar cells (63.2% vs 40.7% [1]).

In IBSCs an electron–hole pair is generated by two mechanisms: the absorption of one photon whose energy is higher than E_G (arrow 3 in Fig. 1), and the absorption of two sub-bandgap photons whose energies are higher than E_H (arrow 1) and E_L (arrow 2) via two pumping-processes through the IB. The energy reference within the IB for defining E_L and E_H is assumed to be at the center of the intermediate band. On the other hand, in devices implemented with quantum dots (QDs) as it will be our case, the IB is considered to emerge from the fundamental energy level associated to the confined electrons and expected to be narrow and even reduced to a degenerated energy level if QDs are far apart. The isolation of the IB from the metal contacts through the emitters implies that the output voltage is proportional to the difference between the quasi-Fermi level of electrons and the quasi-Fermi level of holes, E_{FC} and E_{FV} respectively. Hence, as in a conventional solar cell, the open-circuit voltage (V_{OC}) remains limited by the bandgap of the host semiconductor, E_G.

Quantum dots (QDs) are one of the approaches used to implement IBSCs because the energy states of the electrons confined in the dots can lead to the formation of the IB [2]. The IBSC operating principles have already been demonstrated in InAs/GaAs QDs [3–5]. Unfortunately, this material is not the best candidate to implement a high efficiency IBSC because of the GaAs low bandgap, ($\sim$1.42 eV, to be compared to the optimum value, 1.9 eV [1]). Furthermore, in this material, it has been obtained experimentally a low value for E_L, which leads to undesired thermal escape of electrons between the IB and the CB at room temperature. Thus, there is interest in shifting towards barrier materials with higher bandgaps [6] and higher E_L.

In this respect, IBSCs based on InAs/AlGaAs QDs have been considered as good candidates. This QD system has been studied, providing encouraging results such as a larger E_L [6], the generation of two-photon below bandgap photocurrent and voltage-up conversion of low-energy photons [7]. Unfortunately, the use of low temperature has still been required in order to decrease thermal escape and obtain some of these results.

In order to work towards the demonstration of the IBSC operating principles at RT, we have manufactured InAs QDs based on AlGaAs barriers with a concentration of aluminum slightly larger than the one used in the works cited above (Al content of 30% instead of 25%). These cells have been characterized by photocurrent measurements and current–voltage curves under concentrated white-light illumination and the results will be shown in following sections.

* Corresponding author. Tel.: +34 914533556; fax: +34 915446341.
E-mail address: esther.lopez@ies-def.upm.es (E. López).

http://dx.doi.org/10.1016/j.solmat.2015.12.031
0927-0248/

2. Material and methods

2.1. InGaAs/AlGaAs solar cell

The solar cells studied in this work were grown on 350 μm thick n^+-GaAs substrates by molecular beam epitaxy (MBE) at the University of Tokyo. The layer structure of these samples is shown in Fig. 2. Two different types of samples were manufactured: a sample with 25 layers of InGaAs/$Al_{0.3}Ga_{0.7}As$ QDs in the region labeled as "Middle", and a reference sample without QDs in which this middle region consists of $Al_{0.3}Ga_{0.7}As$. In both samples this layer has no intentional doping and is sandwiched between conventional p (2×10^{18} cm^{-3}) and n (8×10^{16} cm^{-3}) type $Al_{0.3}Ga_{0.7}As$.

A back surface field layer ($Al_{0.75}Ga_{0.25}As$ n-type doped 1×10^{17} cm^{-3}) was grown on top of a 250 nm n^+-GaAs buffer layer (1×10^{18} cm^{-3}). A window layer ($Al_{0.75}Ga_{0.25}As$ p-type doped 5×10^{18} cm^{-3}) was grown on top of the emitter, followed by a p^+-GaAs (2×10^{19} cm^{-3}) contact layer. Finally, metal contacts were deposited by thermal evaporation both on the back (AuGe/Ni/Au) and the front (Cr/Au) sides of the device.

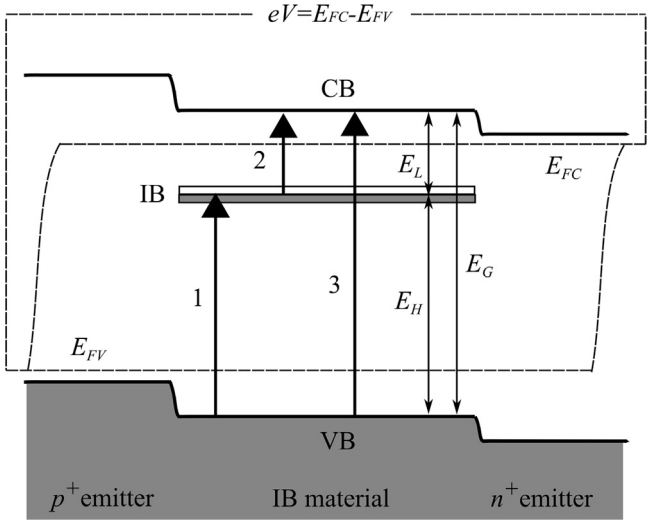

Fig. 1. Band diagram of an IBSC under operating conditions (illumination and forward bias). The three absorption processes and the relationship between the output voltage, V, and the quasi-Fermi levels of electrons and holes, E_{FC} and E_{FV}, are shown.

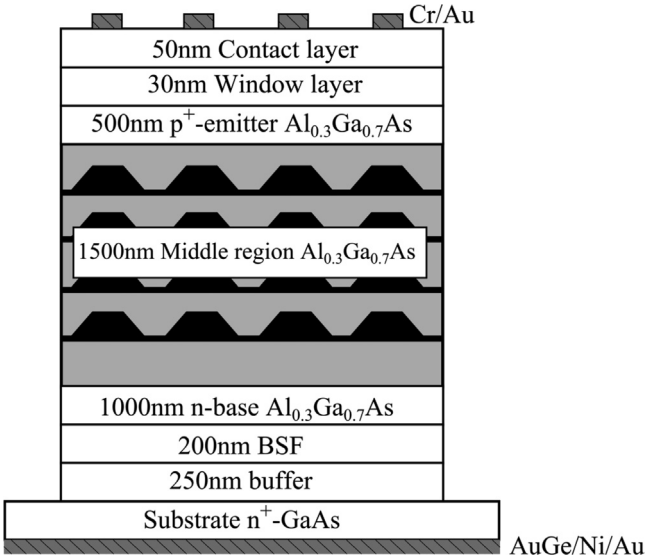

Fig. 2. Layer structure of the QDs solar cell studied in this work. The middle region consists of 25 layers of InGaAs/$Al_{0.3}Ga_{0.7}As$ QDs spaced 60 nm. In the case of the reference cell, the middle region consists of $Al_{0.3}Ga_{0.7}As$ with no QDs.

InGaAs QDs were fabricated by the growth interruption technique. Hence, the QDs were formed during the growth interruption after 10.5 MLs of InGaAs were deposited, at high growth rate of ~1 ML/s, on intrinsic $Al_{0.3}Ga_{0.7}As$ spacers of 60 nm [8,9]. Due to the doping level and the thickness of the layers in Fig. 2, the QDs were located inside the space-charge region of the solar cell. Hence, as described in [10], in equilibrium, it is warranted that some QD layers are partially filled with electrons at the prize that some other layers are either filled or emptied of electrons.

2.2. Photocurrent measurements

The photocurrent measurements are performed at RT by illuminating the samples with sub-bandgap photons with energy in the range from 0.2 eV to 1.4 eV (the $Al_{0.3}Ga_{0.7}As$ bandgap is around 1.8 eV [11]). Therefore, the photocurrent must be generated by optical transitions that involve intermediate levels, which exist, in principle, only in the solar cells with QDs. Hereinafter, we will refer to these levels as IB.

The measured photocurrent responds to the monochromatic light that comes from the output of a 1/4 m monochromator. Inside the monochromator, the light of a 100 W halogen lamp is diffracted and, at the output, appropriate optical filters are placed to guarantee the monochromaticity of the photon beam. In order to maximize the measured photocurrent, the output monochromatic beam is concentrated as much as possible with a parabolic mirror, guaranteeing that the light spot covers the total area of the solar cells (0.032 cm^2). The spectral photon flux is in the range of 4.3×10^{14}–3.7×10^{20} $m^{-2}\,s^{-1}\,nm^{-1}$ for photons with energy above 0.9 eV and is measured for each energy with a calibrated Newport photodetector. This calibration also allows measuring the external quantum efficiency of the cell (EQE) for photon energies above 0.9 eV. It can be assumed that for energies lower than 0.9 eV the photon flux that illuminates the solar cells is lower than the values of this range but no absolute calibration has been possible.

The intensity of the monochromatic beam is modulated at 33 Hz using an optical chopper, and the alternate photocurrent generated by the cell in response to this illumination is measured with a lock-in amplifier. For each of the two samples studied in this work, this photocurrent is measured under two different operation conditions, to know, with and without illumination by means of a continuous-wave (cw) laser diode of 1.32 eV (energy lower than E_G). The latter illumination alone produces a continuous photocurrent density of 0.52 mA/cm^2 in the QD solar cell. This photocurrent density is equivalent to the current density generated by this solar cell when illuminated by 0.5 suns (resulting from integrating the EQE of the cell for photons with energy higher than 0.9 eV with ASTM-G173-0 spectrum). During all photocurrent measurements, samples were biased at 0 V.

2.3. Concentration measurements

The short-circuit current density (J_{SC}) vs. V_{OC} curves under different levels of illumination are measured at RT using the experimental technique described in [12]. In this technique, the light of a Metz Mecablitz 54 MZ-3 xenon flash lamp is concentrated by a CaF_2 lens to illuminate the cells with different irradiances during the time of the flash discharge. This time is approximately 20 ms long, although 90% of the energy is discharged approximately within the first 5 ms. Two flash pulses are used to obtain the J_{SC}–V_{OC} pairs. During the first pulse, samples are biased at 0 V using a 4-wire Keithley source meter, so that J_{SC} values at different irradiances are obtained as the intensity of the light of the flash decays. During the second pulse, samples operate at open-circuit, so that V_{OC} values at